

Electronic Supplementary Material (ESI)

Highly Dispersed Copper Phosphide Nanoparticles Accelerate Electrolytic Water Oxidation Process

Haishun Jiang^{a, b}, Jihua Shi^{a, b}, Xiangyue Liu,^{a, b} Jing Tang*^{a, b}

a Key Laboratory for Analytical Science of Food Safety and Biology, Ministry of Education, College of Chemistry, Fuzhou University, Fuzhou, 350116, P. R. China;

b Fujian Provincial Key Laboratory of Electrochemical Energy Storage Materials, Fuzhou University, Fuzhou, 350108. P. R. China.

Experiment

Electrochemical measurement

The evaluation of hydrogen evolution reaction (HER) and oxygen evolution reaction (OER) performance within the typical three-electrode system in the 1M KOH solution (the actual pH tested was 13.8), and all measurements were carried out on the CHI 920C workstation. The prepared material was used as work electrode (1.5 cm * 0.5cm), the counter electrode was graphite plate (1cm * 3cm * 3mm) and Hg/HgO was used as reference electrode, respectively. Cyclic voltammetry (CV) curves were obtained at scan rate of 20 mV s⁻¹ until the end of two completely overlapping CV curves from -0.22 ~ 0.52V vs. Hg/HgO, Linear sweep voltammetry (LSV) carried out with iR compensation (90%) at a sweep rate of 2 mV s⁻¹ and the potential versus reversible hydrogen electrode (RHE) was calculated by Nernst equation, as follow,

$$E_{\text{vs.RHE}} = E_{\text{vs.Hg/HgO}} + 0.0592 \cdot \text{pH} + 0.098\text{V}$$

Electrochemical impedance measurements were executed in FRA impedance potentiostatic mode from 0.1 HZ to 100K HZ. Besides, double-layer capacitance (C_{dl}) measurements were tested with the scan rate from 10 to 80 mV s⁻¹, where the potential range for HER from -0.65V to -0.75V and OER from 0.15V to 0.25V refer to the Hg/HgO electrode, respectively.

Supplementary Experimental Figures

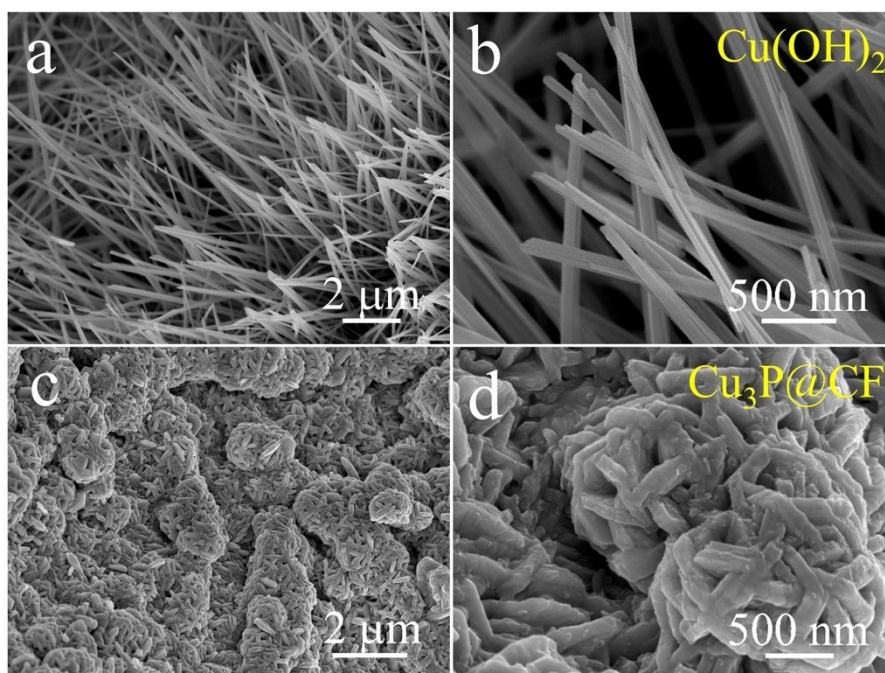


Figure S1. SEM images of $\text{Cu}(\text{OH})_2$ NRs (a, b) on the CF and $\text{Cu}_3\text{P}@CF$ (c, d).

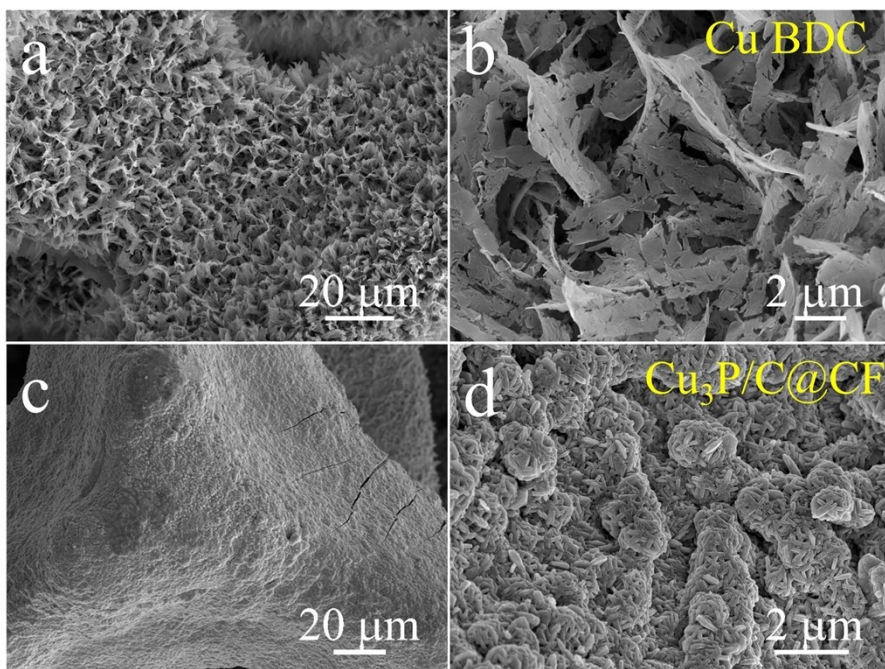


Figure S2. SEM images of Cu MOF nanosheets (a, b) on the CF and (c, d) $\text{Cu}_3\text{P}/C@CF$.

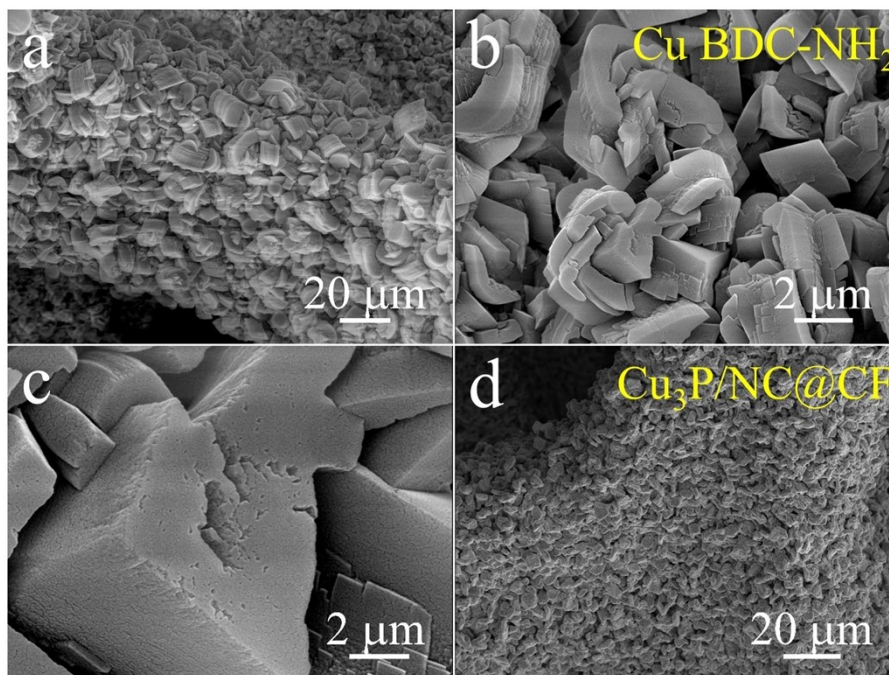


Figure S3. SEM images of Cu MOF-NH₂ (a-c) nanocubes on the CF and Cu₃P/NC@CF (d).

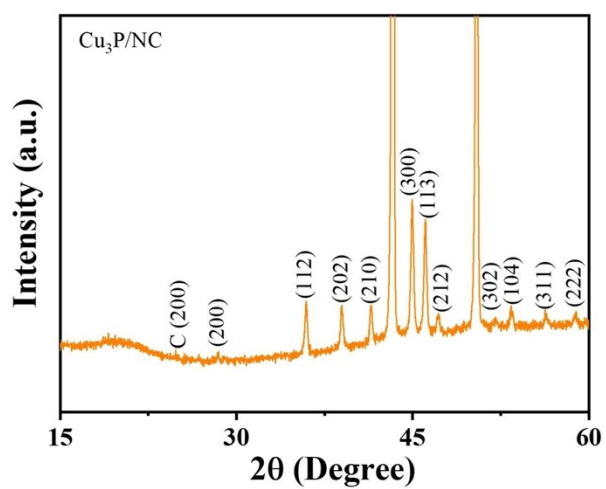


Figure S4. The XRD pattern of Cu₃P/NC@CF corresponding to the crystal plane.

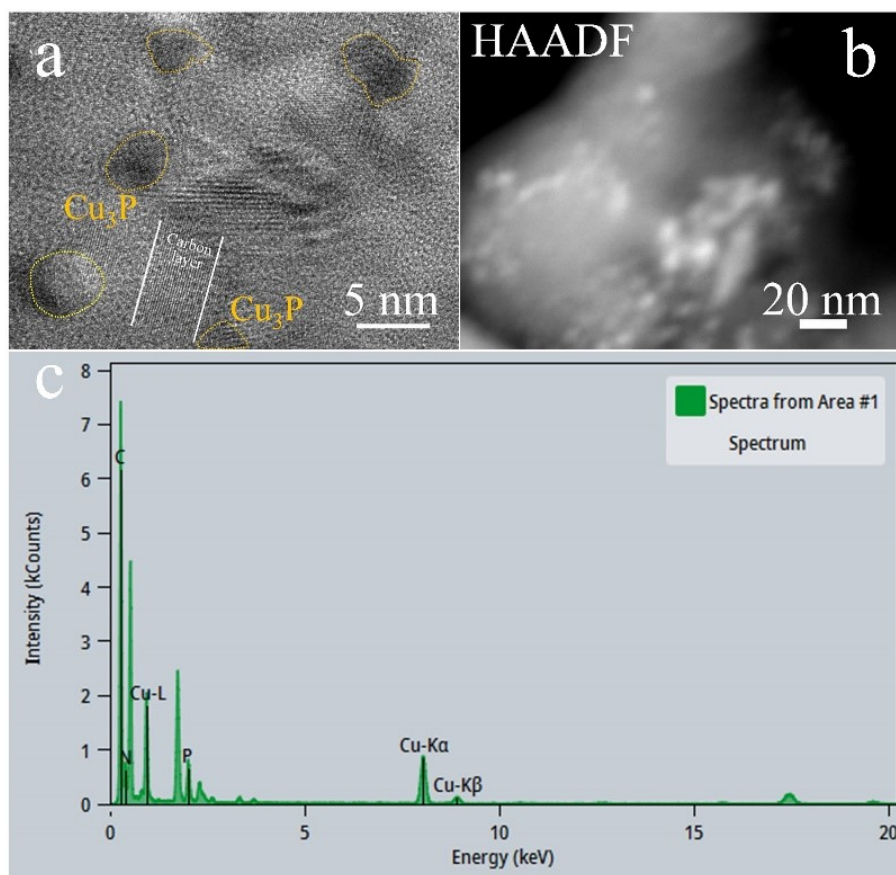


Figure S5 Cu₃P/NC@CF (a) TEM image (The yellow circle contains the isolated Cu₃P NPs and the Cu₃P is surrounding by Carbon matrix), (b) HAADF-TEM image (c) and corresponding with EDX element mapping.

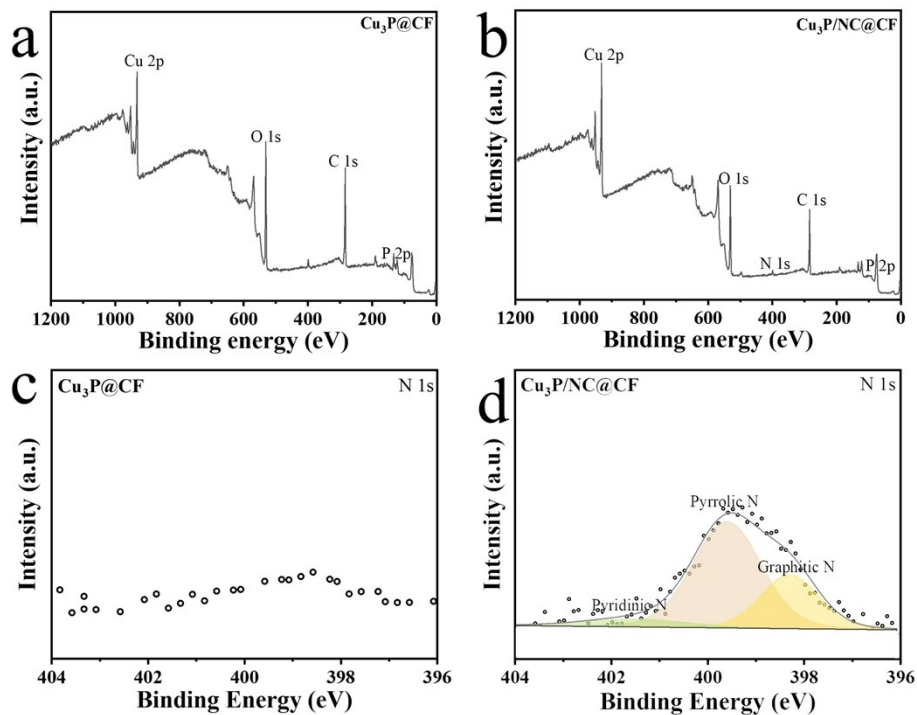
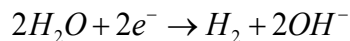


Figure S6. (a) and (b) The XPS full spectra of $\text{Cu}_3\text{P@CF}$ and $\text{Cu}_3\text{P/NC@CF}$, (c) and (d) the N1s fine resolution of $\text{Cu}_3\text{P@CF}$ and $\text{Cu}_3\text{P/NC@CF}$, respectively.

Generally, the HER process is a two-electron process in alkaline solution in individual Volmer-Heyrovsky or Volmer-Tafel mechanism, details of the above-discussed mechanism and the rate-determining step (RDS, Tafel slope value) are equated as below,



$$b = \frac{2.303RT}{\alpha F} \approx 120 \text{ mV} / \text{dec}$$



$$b = \frac{2.303RT}{(1+\alpha)F} \approx 40 \text{ mV} / \text{dec}$$



$$b = \frac{2.303RT}{2F} \approx 30 \text{ mV} / \text{dec}$$

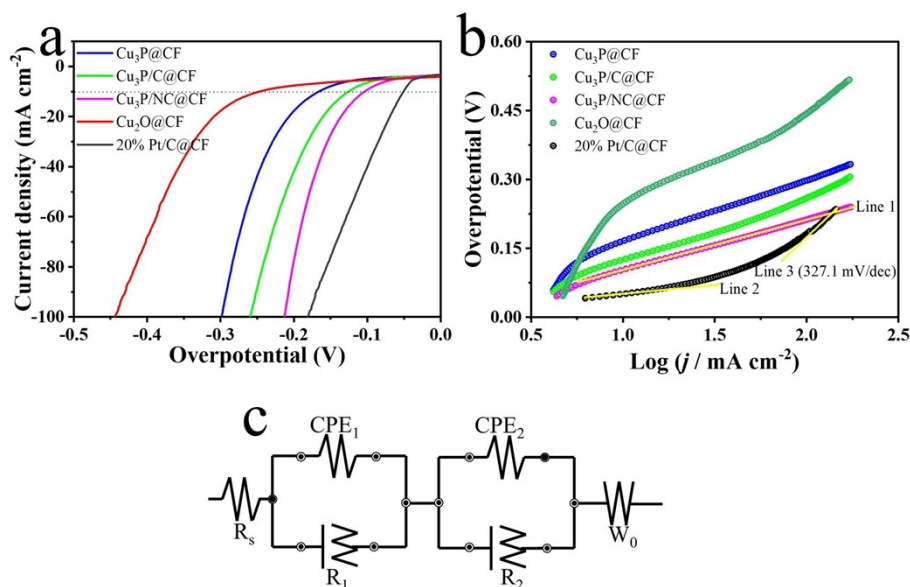


Figure S7. (a - b) LSV curves and Tafel slopes of Cu₃P@CF, Cu₃P/C@CF, Cu₂O@CF and 20% Pt/C@CF, (c) Equivalent circuit model that contains the electrolyte resistance (R_s), constant phase element (CPE_{1,2}) and charge transfer resistance (R_{1,2}).

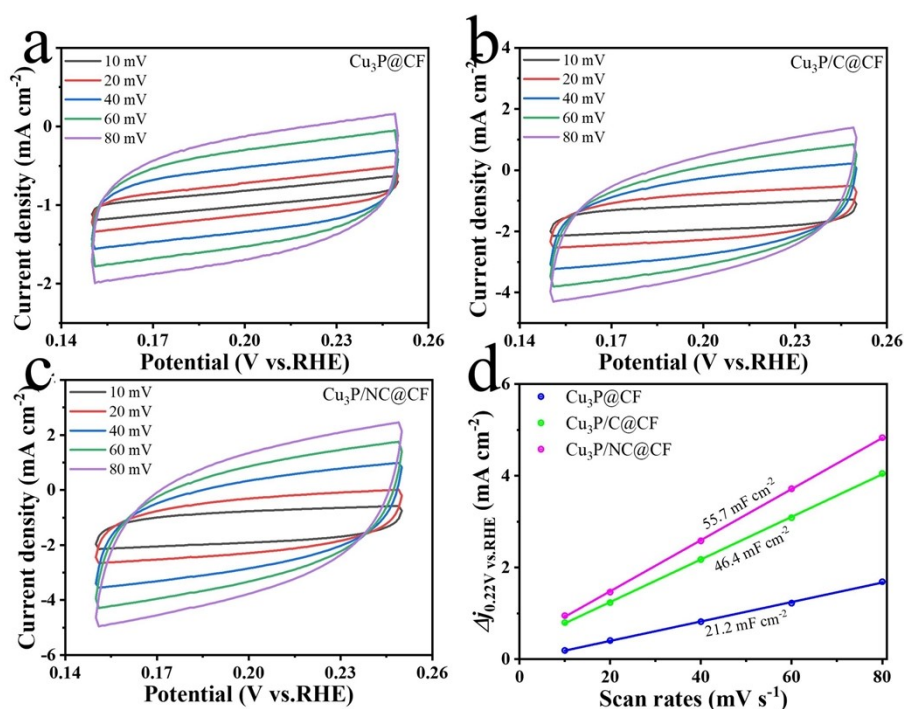


Figure S8. (a - c) CV curves of Cu₃P@CF, Cu₃P/C@CF and Cu₃P/NC@CF at the scan rates from 10 to 80 mV s⁻¹, (d) and the corresponding capacitive currents at 0.22V vs.RHE as a linear fitting function.

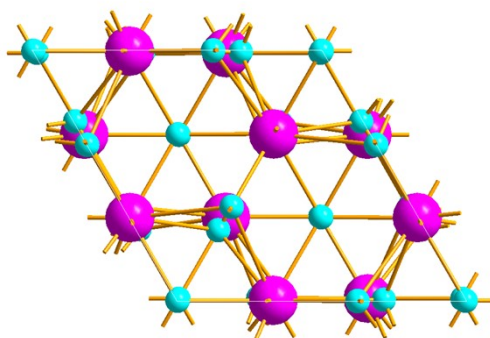


Figure S9. The crystal structure of Cu₃P (Atoms: Turquoise Cu and Pink P. The Volume=299.6Å³).

As for accurate active sites it is difficult to determine, in Fig. S9, the Monoclinic crystal cell of copper phosphide contains 4 Cu-P constituted. So, the definition of active sites that obtained a close value relevant with real number of atoms per real surface area. We get some experience from previous works^{S1}.

Number of active sites per square specific surface area:

$$N_{\text{active sites}} = \left(\frac{4 \text{ (atoms active center) unit cell}^{-1}}{299.6 \text{ \AA}^3 \text{ unit cell}^{-1}} \right)^{\frac{2}{3}} = 5.68 \times 10^{14} \text{ atoms} \quad \text{Eq.}$$

S4

#active sites per real surface area:

$$A_{\text{ECDSA}}^{\text{Cu}_3\text{P}} = \frac{21.2 \text{ mF cm}^{-2}}{40 \text{ \mu F cm}^{-2} \text{ per cm}^2} = 503 \text{ cm}^2 \quad \text{Eq. S5}$$

$$A_{\text{ECDSA}}^{\text{Cu}_3\text{P/C}} = \frac{46.4 \text{ mF cm}^{-2}}{40 \text{ \mu F cm}^{-2} \text{ per cm}^2} = 1160 \text{ cm}^2 \quad \text{Eq. S6}$$

$$A_{\text{ECDSA}}^{\text{Cu}_3\text{P/NC}} = \frac{55.7 \text{ mF cm}^{-2}}{40 \text{ \mu F cm}^{-2} \text{ per cm}^2} = 1392 \text{ cm}^2 \quad \text{Eq. S7}$$

Convert the total hydrogen calculated from the current density, as follows,

$$H_2(\text{per mA/cm}^{-2}) = \left(j \frac{\text{mA}}{\text{cm}^2} \right) \left(\frac{1 \text{ C s}^{-1}}{1000 \text{ mA}} \right) \left(\frac{1 \text{ mol e}^{-1}}{96485.3 \text{ C}} \right) \left(\frac{1 \text{ mol H}_2}{2 \text{ mol e}^{-1}} \right) \left(\frac{6.022 \times 10^{23} \text{ H}_2 \text{ mol}}{1 \text{ mol H}_2} \right)$$

$$= 7.8 \times 10^{14} \text{ H}_2 \text{ s}^{-1} \text{ cm}^{-2} \text{ per (mA cm}^{-2}) \quad \text{Eq. S8}$$

Turnover frequency calculation of catalysts as follows^{S2},

$$\text{TOF per sites} = \frac{\text{total oxygen turnovers cm}^{-2} \times \text{geometric area}}{\text{active sites cm}^{-2} \times \text{geometric area}} \quad \text{Eq. S9}$$

Converted to a new TOF calculation formula according to the definition formula Eqs.9

$$\text{TOF} = \frac{5.68 \times 10^{14} \text{ H}_2 \text{ s}^{-1} \text{ cm}^{-2} \text{ per (mA cm}^{-2}) \times |j|}{7.8 \times 10^{14} \text{ atoms} \times A_{\text{ECDSA}}} \quad \text{Eq. S10}$$

At the overpotential of -200 mV, the TOF value of the pristine Cu₃P@CF is 0.0258 H₂ s⁻¹, but the Cu₃P/C@CF and Cu₃P/NC@CF get a better value is 0.0259 H₂ s⁻¹ and 0.0406 H₂ s⁻¹.

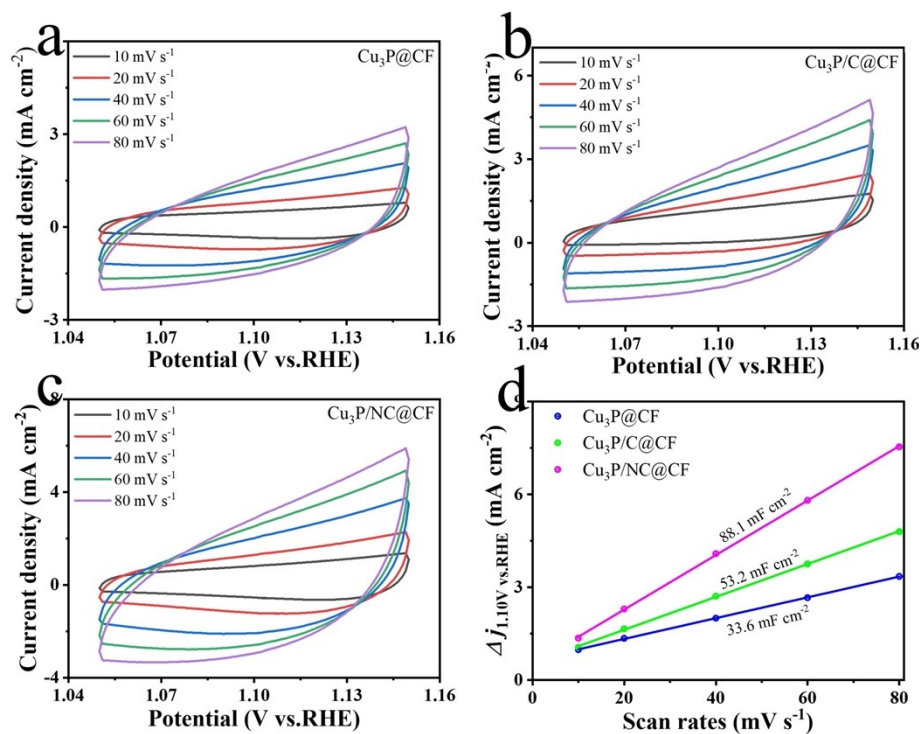


Figure S10. CV curves of $\text{Cu}_3\text{P}@CF$, $\text{Cu}_3\text{P}/C@CF$ and $\text{Cu}_3\text{P}/NC@CF$ at the scan rates from 10 to 80 mV s^{-1} .

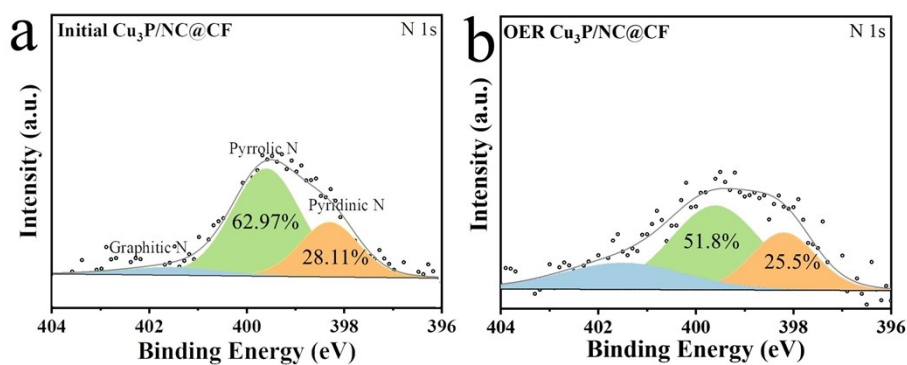


Figure S11. The N 1s XPS spectra resolution of $\text{Cu}_3\text{P}/NC@CF$ before and after OER tested for 36 hours.

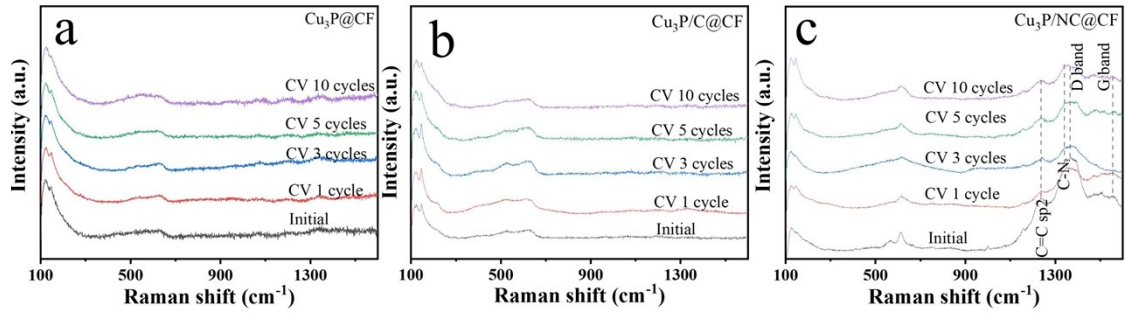


Figure S12. Raman spectra of $\text{Cu}_3\text{P}@CF$, $\text{Cu}_3\text{P}/C@CF$ and $\text{Cu}_3\text{P}/NC@CF$.

Table S1. The Raman shift is 607 cm^{-1} of $\text{Cu}_3\text{P@CF}$, $\text{Cu}_3\text{P/C@CF}$ and $\text{Cu}_3\text{P/NC@CF}$ with CV cycles

Intensity (a.u.)	$\text{Cu}_3\text{P@CF}$	$\text{Cu}_3\text{P/C@CF}$	$\text{Cu}_3\text{P/NC@CF}$
0	1092.11	13837.68	26614.57
CV 1 cycle	1936.39	10627.45	9029.63
CV 3 cycles	2383.06	7699.98	13951.90
CV 5 cycles	1530.71	6484.57	22241.68
CV 10 cycles	1537.81	5197.00	25389.14

Table S2. The Raman shift is 274 cm^{-1} of $\text{Cu}_3\text{P@CF}$, $\text{Cu}_3\text{P/C@CF}$ and $\text{Cu}_3\text{P/NC@CF}$ CV cycles

Intensity (a.u.)	$\text{Cu}_3\text{P@CF}$	$\text{Cu}_3\text{P/C@CF}$	$\text{Cu}_3\text{P/NC@CF}$
0	1905.77	15028.70	10697.88
CV 1 cycle	1753.47	12830.83	10495.28
CV 3 cycles	1757.28	9743.06	18266.33
CV 5 cycles	2056.08	8282.70	25675.30
CV 10 cycles	2146.09	6102.84	28597.23

The Oxygen evolution reaction mechanism alkaline solution, as follows^{S3}:

- i) $M + OH^- \rightarrow M-OH + e^-$ Eq. S11
- ii) $M-OH + OH^- \rightarrow M-O + e^- + H_2O$ Eq. S12
- iii) $M-O + OH^- \rightarrow M-OOH + e^- + H_2O$ Eq. S13
- iv) $M-OOH + OH^- \rightarrow M-OO + e^- + H_2O$ Eq. S14
- v) $M-OO + OH^- \rightarrow M + O_2$ Eq. S15

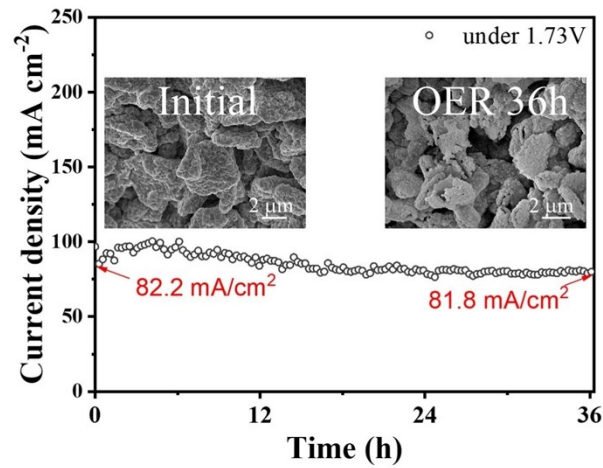


Figure S13. Chronopotentiometric measurement of Cu₃P/NC @CF and the insert diagrams are the SEM images before and after water splitting for 36 hours in 1M KOH solution.

Supplementary References

- [S1] E. J. Popczun, J. R. McKone, C. G. Read, A. J. Biacchi, A. M. Wiltrout, N. S. Lewis and R. E. Schaak, *J. Am. Chem. Soc.*, 2013, 135, 9267–9270.
- [S2] T. Tian, H. Gao, X. Zhou, L. Zheng, J. Wu, K. Li and Y. Ding, *ACS Energy Lett.*, 2018, 3, 2150–2158.
- [S3] H. Sun, Z. Yan, F. Liu, W. Xu, F. Cheng and J. Chen, *Adv. Mater.*, 2020, 32, 1–18.